

# <sup>1</sup>H nuclear magnetic resonance characterization of internal motions in the amorphous phase of low-density polyethylene

D. Doskočilová, B. Schneider, J. Jakeš, P. Schmidt and J. Baldrian

*Institute of Macromolecular Chemistry, Czechoslovak Academy of Sciences, 162 06 Prague 6, Czechoslovakia*

and I. Hernández-Fuentes and M. Caceres Alonso

*Departamento de Química Física, Facultad de Ciencias Químicas, Universidad Complutense, Madrid 3, Spain*

*(Received 3 December 1985; revised 28 February 1986)*

<sup>1</sup>H nuclear magnetic resonance (n.m.r.) spectra of low-density polyethylene, static and with magic-angle rotation (MAR), were measured in the range 270–385 K. The amorphous component of the static <sup>1</sup>H n.m.r. spectrum was obtained by subtraction of the crystalline component based on crystallinity determination by X-ray and infra-red methods. The amorphous line is narrowed by more than an order of magnitude by MAR, proving the spatially anisotropic character of internal motion. The temperature dependence of the MAR n.m.r. linewidth corresponds to  $\Delta E = 7.5 \text{ kcal mol}^{-1}$ , which is ascribed to rapid small-scale conformational motions. The static amorphous lineshape could be fitted by the convolution of the MAR n.m.r. line with an orientation-dependent dipolar broadening function by adjustment of a single parameter  $A_0$  characterizing the width of the dipolar broadening. The amorphous lineshape can be described by assuming the presence of only a single amorphous phase. The relation of  $A_0$  to the rigid lattice second moment, as a measure of spatial hindrance, is discussed and the length of the flexible subchain is estimated.

(Keywords: polyethylene; dynamics; motional hindrance; <sup>1</sup>H nuclear magnetic resonance)

## INTRODUCTION

In previous communications from this laboratory several systems with spatially hindered internal motions were investigated by a combination of the methods of <sup>1</sup>H n.m.r. static lineshape analysis and <sup>1</sup>H magic-angle rotation (MAR) n.m.r. In static <sup>1</sup>H n.m.r. spectra, chemically crosslinked networks (poly(ethylene oxide), polystyrene)<sup>1,2</sup> swollen to equilibrium in various solvents exhibit lineshapes with very sharp peaks and very broad wings which can be reduced to much narrower Lorentzian lines by magic-angle rotation (MAR n.m.r.). These lineshapes have been analysed in terms of the lineshape equation<sup>3</sup>:

$$I(\omega - \omega_0) = \int_0^{\pi/2} \int_{-\infty}^{\infty} \left[ R(\omega - \omega_1) S\left(\frac{\omega_1 - \omega_0}{|3 \cos^2 \theta - 1|}\right) \times (|3 \cos^2 \theta - 1|)^{-1} \right] d\omega_1 \sin \theta d\theta \quad (1)$$

This is a convolution of the functions  $R$  and  $S$ , where  $\theta$  is the angle between a specified direction (e.g. inter-crosslink vector) and the static magnetic field. The function  $R$  corresponds roughly to the MAR n.m.r. line and is governed by rapid conformational motions; the function  $S$  corresponds to a dipolar broadening function

where the width (but not the shape) depends on the orientation ( $\theta$ ) of the specified direction with respect to the magnetic field; thus the angular dependence of  $S$  may be separated from the shape (Gaussian, Lorentzian or other) and from the characteristic width,  $2A_0$ , defined for  $\theta = \pi/2$ .

For equilibrium-swollen chemically crosslinked networks, the parameter  $A_0$  was found to be almost temperature-independent and to exhibit a linear dependence on the degree of crosslinking<sup>1,2</sup>. A relation between  $A_0$  and the conformation of the inter-crosslink chain could be established, indicating that this conformation is similar to that of the free chain of equal length<sup>2</sup>.

Besides swollen chemically crosslinked networks, an attempt was made to apply the same type of analysis to the <sup>1</sup>H n.m.r. signal of the amorphous phase of polyethylene (PE)<sup>4</sup>. The previously most frequently used procedure for analysing the static <sup>1</sup>H n.m.r. lineshape of semicrystalline PE was that of Bergmann<sup>5,6</sup> assuming the presence of two amorphous phases. In this analysis, the shape of the crystalline component was derived from experiment, the lineshapes of the two amorphous components were postulated, and their widths, relative amounts and content of crystalline phase were adjusted. In a later communication, Bergmann<sup>7</sup> demonstrated that the crystalline component can be suppressed by a spin-locking experiment, and the resulting free induction decay (FID) corresponding to the amorphous phase

analysed as composed not of two components but of a continuous distribution of states with continuously varying correlation times. In our previous communications<sup>4,8</sup> we have demonstrated that the width of the amorphous line component of PE can be reduced by more than an order of magnitude by magic-angle spinning at a spinning rate of the order of 1 kHz. This contradicts both the above procedures, and requires description of the amorphous line component by a convolution of a narrow lineshape function as revealed by MAR, with a dipolar broadening function. The increase of the intensity of the MAR n.m.r. line, at constant linewidth, with increasing spinning rate<sup>8</sup> shows that the dipolar broadening function cannot be simple, but must have the character of a heterogeneous distribution of lines of continuously increasing width, but all of them governed by a correlation frequency  $\nu_c \leq 10^3$ . Such a distribution can hardly be visualized as a distribution of phases. However, it can be easily correlated with a model of spatially hindered internal motion, advocating analysis in the sense of equation (1).

Using the shape of equation (1), with both *S* and *R* Lorentzian, a satisfactory fit was obtained for room-temperature spectra of a series of both high-density and low-density PE samples (HDPE and LDPE) of widely differing crystallinity assuming the presence of only a single amorphous phase<sup>4</sup>. At the same time, the parameters of the narrow lineshape function, obtained from MAR n.m.r. spectra, as well as the parameters of the dipolar broadening function obtained by lineshape fitting, differed only little in the series of samples with widely differing crystallinity, indicating homogeneity of the amorphous phase, and the similarity of its dynamics and motional restrictions in the measured series. This result is in good agreement with the present notions<sup>9</sup> derived predominantly from small-angle neutron scattering (SANS) experiments about the conformation of polymer chains in the amorphous phase of semicrystalline polymers, which is supposed to be little perturbed from its random coil state by the presence of the crystallites.

In the present study, in order to investigate the motional characteristics of the amorphous phase of PE in greater detail, we measured the temperature dependence of static and MAR <sup>1</sup>H n.m.r. spectra of a sample of PE with a high content of amorphous phase. We wished to determine the temperature dependence of the shape of the n.m.r. signal of the amorphous phase with sufficient accuracy and with a minimum of *a priori* assumptions. For correct subtraction of the crystalline component, the temperature dependence of the crystallinity of our sample was determined independently by X-ray and infra-red (i.r.) methods.

## EXPERIMENTAL

The studied sample was Lupolen (BASF) 3020 D, of density  $0.929 \text{ g cm}^{-3}$ ,  $[\eta] = 1.3$ , melting index  $0.2 \text{ g/10 min}$ . According to <sup>13</sup>C n.m.r. analysis<sup>10</sup> (JEOL FX-60 spectrometer, 15 MHz), this sample contains 10 branches per 1000 carbons, with the majority of the branches longer than two carbons.

For measurements of broad-line (BL) <sup>1</sup>H n.m.r. spectra, this sample was used without further treatment in the form of a machined cylinder 5.5 mm in diameter. For measurements this was placed in a sealed glass cell of

outer diameter 6.25 mm. For measurements of <sup>1</sup>H MAR n.m.r. spectra, at temperatures up to 65°C, a rotor of outer diameter 6.25 mm was machined from a block of the measured material. For the measurement of <sup>1</sup>H MAR n.m.r. spectra at temperatures above 65°C, small pieces of the measured material prepared by cutting were filled into a glass rotor.

Measurements of i.r. spectra were made either with lathe turnings of thickness 0.03 mm, or with cut platelets of thickness 1 mm. In the process of cutting, these samples acquired some degree of orientation, which was removed by heating to 391–393 K and slow cooling to room temperature. The isotropy of the samples was checked by measurements with polarized i.r. radiation. For variable temperature measurements, the samples of both types of thickness were heated in a Perkin–Elmer heating cell in the range of 305–385 K and cooled in a cell of our own construction<sup>11</sup> in a stream of cold nitrogen in the range 270–305 K. For measurements of X-ray diffraction, 1 mm thick samples were heated in a stream of hot air in the range 296–365 K.

<sup>1</sup>H n.m.r. spectra were measured on a JEOL JNM-3-60 spectrometer at 60 MHz in the continuous-wave (CW) BL mode with a modulation of 35 Hz. As the BL n.m.r. spectra of the measured sample are characterized by a very sharp peak and very broad wings, the shape of the spectrum in the whole range cannot be measured correctly with a single set of instrumental parameters. Therefore, these spectra were measured with three different combinations of intensity of the r.f. field and of the a.f. modulation selected so that the measurement with the strongest r.f. and a.f. fields yielded reliable shapes of the wings, and the measurement with the weakest r.f. and a.f. fields yielded a correct shape of the peak. The measurement with each set of conditions was repeated six times, the six derivative spectra were digitized, numerically integrated, symmetrized and added by a TN 4000 spectral analyser (Tracor Northern). The final lineshape to be analysed was constructed from the three experimental regimes so that the central part of the line (down to about 10% of maximum intensity) was taken from the measurement with the weakest r.f. and a.f. fields, the wings from the measurements with the strongest r.f. and a.f. fields, and the intermediate part from the intermediate measurements. Intensities were normalized so as to coincide at the  $H - H_0$  values corresponding to 10% and 2% of maximum peak intensity\*.

<sup>1</sup>H MAR n.m.r. spectra were measured on the same spectrometer, with a MAR n.m.r. probe of our own construction<sup>12</sup>. Up to 40°C these spectra were measured in the derivative (BL) mode, at temperatures between 40 and 80°C in both the BL and high-resolution (HR) modes, and at the highest temperatures in the HR mode only. The rotors machined from PE were spun at 5 kHz, the glass rotors at 3 kHz.

I.r. spectra were measured on a Perkin–Elmer 580 B spectrometer, connected on-line with the TN 4000 spectral analyser.

Wide-angle X-ray diffraction was measured on a Hilger and Watts powder diffractometer.  $\text{CuK}\alpha$  radiation was

\* It was verified that even with *FT* spectra obtained by means of a pulse spectrometer, a similar procedure is necessary to obtain correct lineshapes with this kind of sample. Because of the sophisticated mathematical procedures, *FT* spectra are even more liable to the appearance of artefacts than CW BL spectra.

monochromatized by Ni foil and recorded by means of a scintillation counter; an amplitude analyser was used. Small-angle X-ray scattering was measured in a Kratky camera. Radiation, monochromatization and recording were the same as with wide-angle diffraction.

*Determination of crystallinity*

For the determination of crystallinity by means of wide-angle X-ray diffraction, the distribution of intensity was measured in the range of angles 7° to 35°. The obtained diffractograms were analysed with the assumption of symmetrical profiles (Pearson VII) both for the crystalline reflections 110 and 200, and for the amorphous halo<sup>13</sup>. Crystallinity was determined from their integrated intensities according to ref. 14. The small-angle scattering curve was corrected to a point cross-section of the primary beam. The long period was determined from the position of the reflection by means of the Bragg equation.

The i.r. determination of the temperature changes of crystallinity was based on absorbance measurements in the band maxima at 730 cm<sup>-1</sup> (samples of 0.03 mm thickness) and at 1890 cm<sup>-1</sup> (samples of 1 mm thickness). Both these bands are assigned<sup>15,16</sup> to the crystalline phase of PE. For absorbance determination, the band at 730 cm<sup>-1</sup> was separated from the band at 720 cm<sup>-1</sup> assuming Lorentzian lineshapes; the band at 1890 cm<sup>-1</sup> was evaluated by means of the baseline method. The obtained experimental values of i.r. band intensities were related to the crystallinity values obtained from X-ray diffraction by means of a least-squares adjustment of all experimental points to a curve described by a polynomial of degree 5 (Figure 1).

*Lineshape analysis*

The n.m.r. spectra constructed from experimental spectra measured at different r.f. and a.f. field strengths as described above were analysed by least-squares adjustment with calculated spectra obtained as follows.

The shape of the crystalline component of the spectrum was taken from Bergmann<sup>5</sup>. His tabulated values of the derivative spectrum were interpolated linearly and then integrated respecting the temperature-dependent horizontal scale factor. The shape of the amorphous component of the spectrum was calculated from equation (1) with Lorentzian shape of function R, and with (a) Gaussian

$$S_G(\omega - \omega_0) = \exp[-(\omega - \omega_0)^2 / A_{0G}^2] / (\pi^{1/2} A_{0G})$$

and (b) Lorentzian

$$S_L(\omega - \omega_0) = A_{0L} / \{ \pi [ (\omega - \omega_0)^2 + A_{0L}^2 ] \}$$

shape of function S. In case (a) the resulting shape is fully characterized by the parameters A<sub>0G</sub> and 2B<sub>G</sub> (characteristic width of Gaussian function S for θ=90°, and width at half-maximum intensity of Lorentzian function R, respectively); in case (b) by 2A<sub>0L</sub> and 2B<sub>L</sub> (width at half-maximum intensity of the Lorentzian functions S at θ=90° and of R, respectively). The two components were then mixed in the ratio corresponding to the content of the crystalline phase read for the respective temperature from the curve shown in Figure 1. In this calculated spectrum the two (or one if B<sub>L</sub> or B<sub>G</sub> was

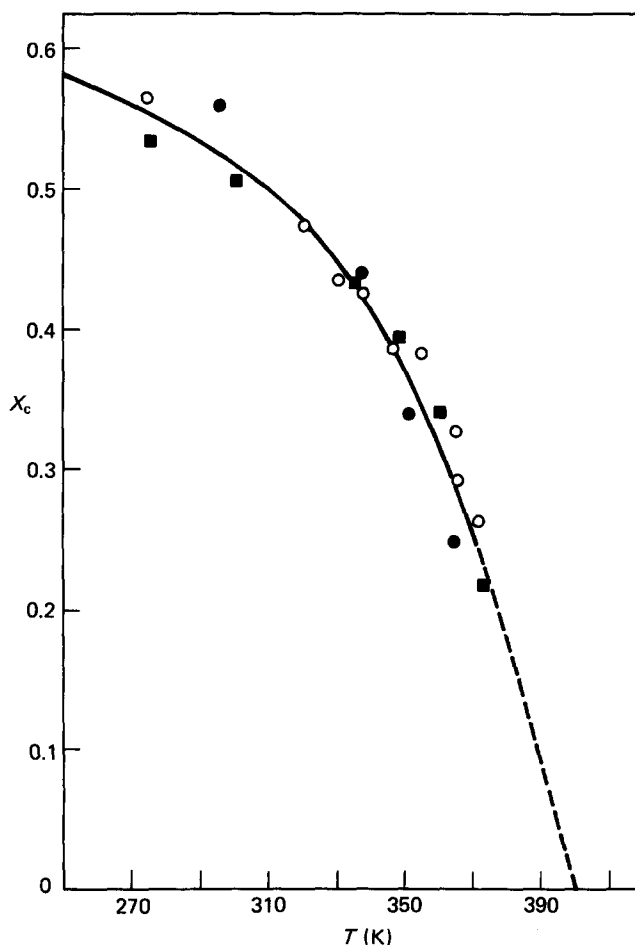


Figure 1 Temperature dependence of fraction of crystalline component X<sub>c</sub> in LDPE sample: ●, X-ray; ○, i.r. band 1890 cm<sup>-1</sup>; ■, i.r. band 730 cm<sup>-1</sup>

fixed at MAR value) width parameters and the vertical scale were adjusted to minimize the expression

$$s = (y_{0,exp} - y_{0,calc})^2 / 2 + \sum_{i=1}^n (y_{i,exp} - y_{i,calc})^2$$

with y<sub>i,exp</sub> obtained from the experimental spectra.

RESULTS AND DISCUSSION

Combined X-ray and i.r. measurements have shown that, in the studied range 270–385 K, the crystallinity of our sample decreases from 56% to only 14.5%. This temperature change is reversible. The decrease is small at low temperatures, but very steep above 330 K (Figure 1). Such 'partial melting' has previously been observed for samples of LDPE<sup>17</sup> and was shown to be accompanied by a large increase in the thickness of the amorphous layers and only a very small increase in the thickness of the crystalline lamellae. In our sample, the long spacing was determined to be 139 Å at room temperature. Thus in the studied temperature range, the dimensions of the amorphous layers are assumed to vary from ~50 Å to several hundred Ångströms.

A static <sup>1</sup>H n.m.r. spectrum of our LDPE sample measured by the CW BL method, with r.f. and a.f. amplitudes carefully adjusted so as to reproduce correctly both the peak and the wings of the line, is shown in Figure 2. The at least two-component character of the spectrum

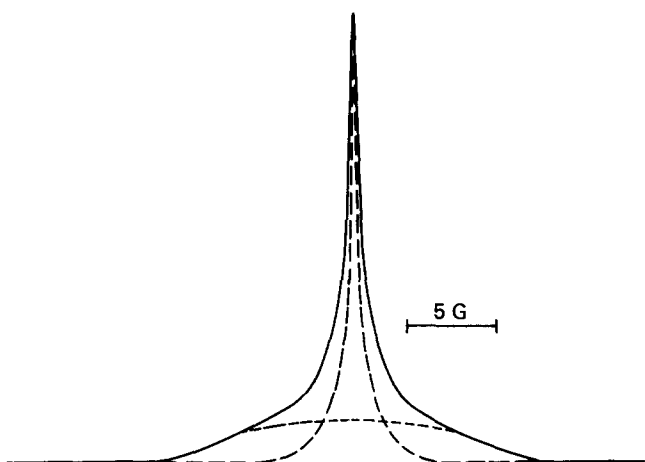


Figure 2 Static <sup>1</sup>H n.m.r. spectrum of LDPE sample, 308 K: —, total lineshape; ----, crystalline component; - · -, amorphous component

is quite pronounced, and the shapes of the crystalline component and of the amorphous component obtained by analysis are also shown. With increasing temperature, the broad line of the crystalline component becomes less conspicuous.

By magic-angle spinning the line of the amorphous component is narrowed by more than an order of magnitude and proportionately increased in amplitude; the line of the crystalline component is too broad to be affected by magic-angle spinning at 3–5 kHz spinning speed. The resulting MAR n.m.r. spectrum has the form of a near-to-Lorentzian shape corresponding to the amorphous phase, with the line of the crystalline component lost in the background. It has been shown in our previous communications<sup>4,8</sup> that the narrowing of the amorphous line component of various PE samples, including Lupolen 3020D, by MAR already takes place at spinning speeds of the order of 1 kHz, and that the limiting linewidth of the MAR n.m.r. line does not depend on spinning speed<sup>8</sup>. This proves the presence of near-static dipolar interactions in the amorphous phase, with a correlation time  $\tau_c \geq 10^{-3}$  s.

The temperature dependence of the MAR n.m.r. linewidth of our LDPE sample is summarized in Figure 3. The narrowing by MAR ranges from one to two orders of magnitude. The widths vary from 2600 Hz to 28 Hz and give a linear dependence in a semilogarithmic plot vs.  $1/T$ . Assuming that the linewidth is proportional to the correlation frequency of internal motions,  $\tau_c$ , the slope of this plot corresponds to an activation energy  $\Delta E$  of 7.5 kcal mol<sup>-1</sup>, with the order of the correlation frequency  $\tau_c$  varying from 10<sup>-6</sup> s at the lowest temperature to 10<sup>-8</sup> s at the highest temperature of the measured range. The  $\Delta E$  value of 7.5 kcal mol<sup>-1</sup> is very near to the value  $\Delta E = 7$  kcal mol<sup>-1</sup> found by Kimmich *et al.* by analysis of  $T_1$  dispersion curves for the  $\gamma$ -process in the amorphous phase of PE<sup>18,19</sup>; this  $\Delta E$  value was related by the authors to two cooperative *trans-gauche* transitions<sup>19</sup>. This comparison corroborates our original assumption<sup>4</sup> that the MAR n.m.r. linewidth is determined by relatively rapid conformational motions. In view of the presence of the near-static dipolar interactions, these rapid conformational motions must be anisotropic in space, i.e. can proceed only over a restricted space angle.

Examples of experimental spectra and of the corresponding calculated spectra obtained by lineshape

fitting in the sense of equation (1), using either a Gaussian or Lorentzian shape for the dipolar broadening function  $S$ , are shown in Figure 4. For the lower temperatures a better fit is obtained with a Gaussian form of  $S$ , whereas for the higher temperatures a Lorentzian form gives a better fit.

The parameters obtained by lineshape fitting are summarized in Table 1. The width parameter  $A_{0G}$  of the Gaussian form of  $S$  can be directly evaluated in terms of second moments<sup>3</sup>. For a comparable evaluation, the width parameter  $A_{0L}$  of the Lorentzian form of  $S$  was transformed to the corresponding  $A_{0G}$  by a procedure previously described<sup>2</sup>. The values in columns 6–9 of Table 1 were obtained with a Gaussian or Lorentzian form of the function  $S$  by fitting of the two parameters  $A_{0G}$ ,  $B_G$  or  $A_{0L}$ ,  $B_L$ ; the values in columns 4 and 5 by fitting of only one parameter,  $A_{0G}$  or  $A_{0L}$ , with a Gaussian or Lorentzian form of  $S$ , respectively, and with  $B_G$  or  $B_L$  fixed at the value of  $B_{MAR}$  derived for the respective temperature from the linear temperature dependence of the MAR n.m.r. linewidth (Figure 3). Values of the r.m.s. errors given in parentheses indicate that, with a Gaussian form of  $S$ , the fit obtained with the one-parameter adjustment is comparable with that obtained with the two-parameter adjustment. The possibility of describing the lineshape of the amorphous component in semicrystalline PE by means of equation (1) with a single adjustable parameter over a broad temperature range confirms our original assumption about the homogeneity of the amorphous phase and about the anisotropic nature of its internal motion.

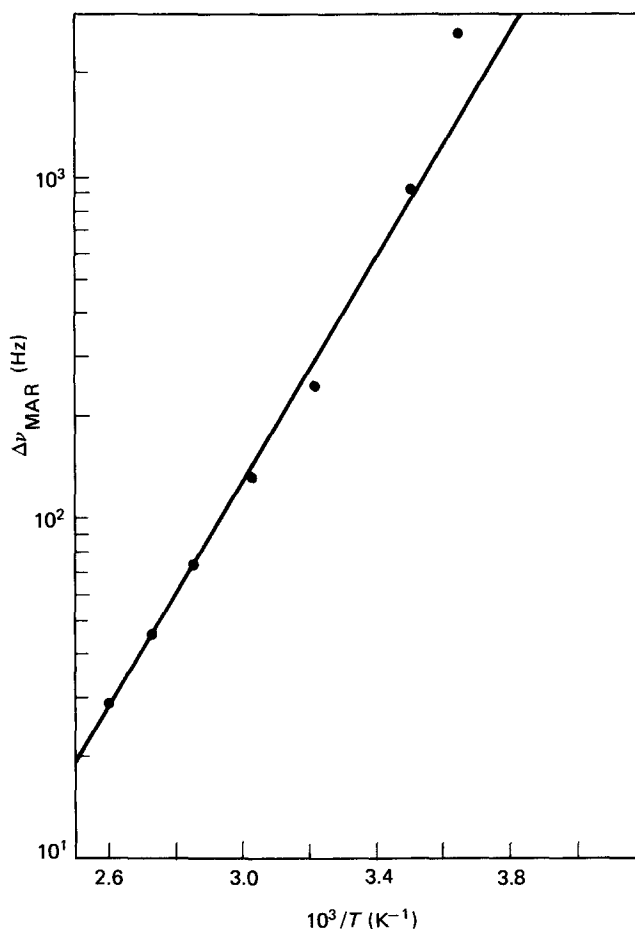


Figure 3 Temperature dependence of MAR n.m.r. linewidth

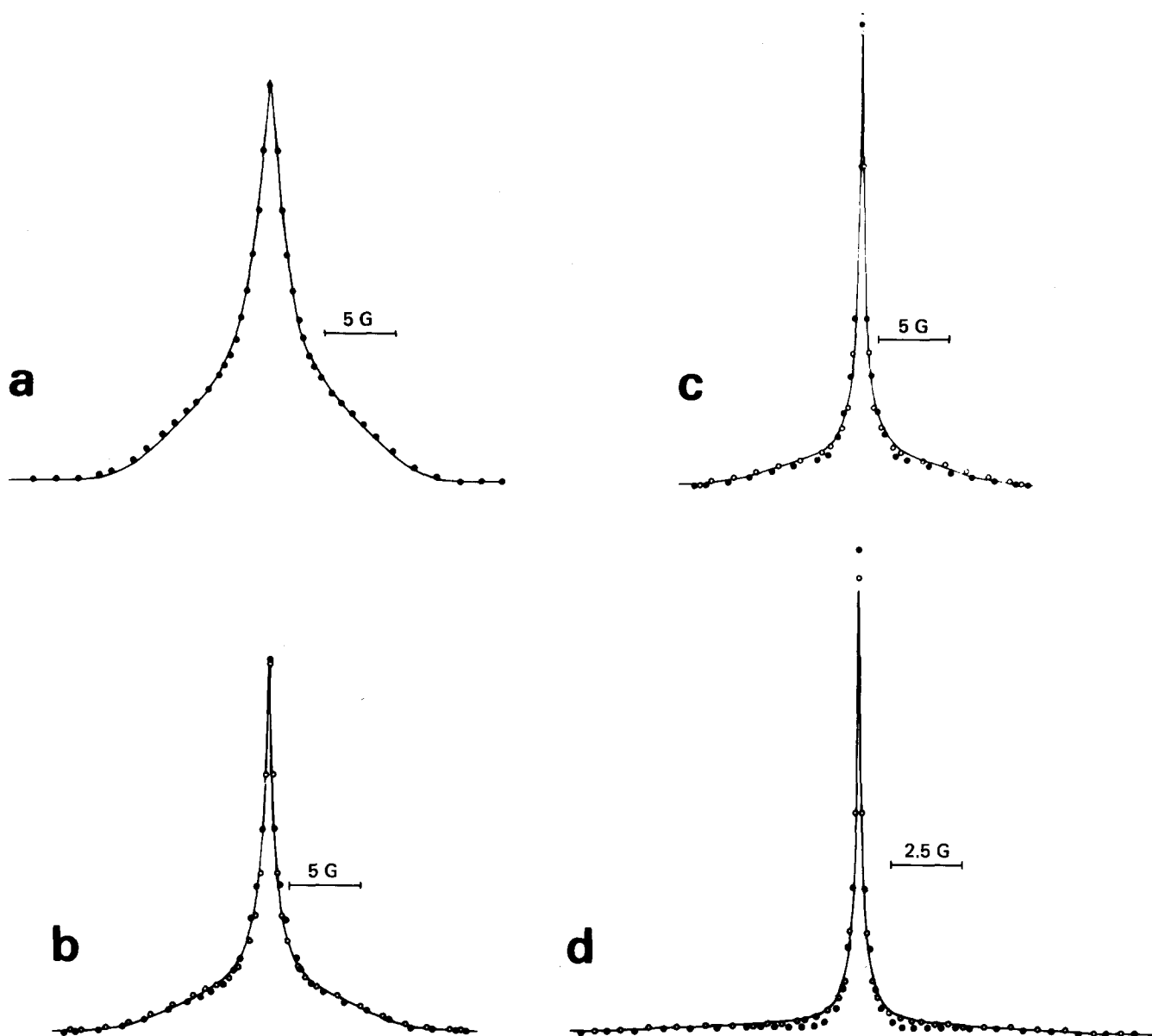


Figure 4 Comparison of experimental static <sup>1</sup>H n.m.r. spectra of LDPE sample and calculated spectra based on equation (1) obtained by adjustment of the parameters *A* and *B*, at (a) 270 K, (b) 308 K, (c) 338 K and (d) 356 K: experimental results (—); spectra calculated with Gaussian (●) or Lorentzian (○) shape of dipolar broadening function *S*

The parameters  $B_G$  obtained by the two-parameter fitting procedure agree very well with the value  $B_{MAR}$  for intermediate temperatures. At the low- and high-temperature extremes,  $B_G$  is somewhat higher than  $B_{MAR}$ . This may be due to the difficulty of measuring correctly the peak region of the overall line in the static spectrum; at the highest temperature, magnetic heterogeneity of the sample could become appreciable. With a Lorentzian form of *S*, the errors are small at high temperatures, but increase towards lower temperatures. At 270 K, a reasonable fit cannot be obtained with the two-parameter adjustment procedure. The parameters  $B_L$  obtained by this procedure are in most cases approximately twice the value of  $B_{MAR}$ . Besides overmodulation and magnetic heterogeneity, this may also stem from the behaviour of the function *S* in the peak region. Thus although the physical meaning of  $B_G$  and  $B_L$  is less well defined than that of  $B_{MAR}$ , in principle it is more correct to use the two-parameter adjustment procedure in order to obtain the best values of  $A_{OG}$  from experimental spectra. Nevertheless, from Table 1 it is evident that the values of

$A_{OG}$  obtained using  $B_G$  and  $B_{MAR}$  differ very little. Even the difference between the  $A_{OG}$  values obtained with Gaussian and Lorentzian shapes of the function *S* is hardly appreciable.

It has been shown in ref. 3 that the dipolar broadening parameter  $A_{OG}$  is related to the residual second moment  $\omega_{2, res}^2$  as  $\omega_{2, res}^2 = \frac{4}{5} A_{OG}^2$ . The relation of the residual second moment to the rigid lattice second moment  $\omega_{2, RL}^2$  is a good quantitative measure of spatial restrictions to internal motions. The ratio of the square roots of these two moments is analogous to the order parameter *S* introduced for partially ordered systems by some authors<sup>20,21</sup>. It should decrease from 1 for rigid systems to 0 for the case of completely isotropic internal motion. The experimentally found ratio of the square roots of the respective second moments is given in Table 1. It is seen to vary from 0.5 to 0.03 in the measured temperature range.

In the 'diffusion in a cone' model, the order parameter is related to the opening angle of the cone<sup>20</sup> as  $S_{cone} = \frac{1}{2}(\cos \alpha_0)(1 + \cos \alpha_0)$ . According to this relation,  $S_{cone}$  decreases very slowly for angles between 0 and 40°

Table 1 Parameters of the amorphous line component of LDPE sample

T (K)	X <sub>c</sub>	One-parameter adjustment			Two-parameter adjustment						
		B <sub>MAR</sub> (mG)	A <sub>0G</sub> (G)	2A <sub>0L</sub> (G)	B <sub>G</sub> (mG)	A <sub>0G</sub> (G)	B <sub>L</sub> (mG)	2A <sub>0L</sub> (G)	A <sub>0G</sub> (G)	$\frac{\omega_{2\text{ res}}}{\omega_{2\text{ RL}}}$	n <sup>a</sup>
270	0.56	202	2.98 (0.868) <sup>b</sup>	3.09 (2.338) <sup>b</sup>	283	2.73 (0.735) <sup>b</sup>	—	—	—	0.509 <sup>c</sup>	5.9
308	0.51	36.4	2.24 (0.616)	2.40 (0.963)	33.2	2.25 (0.613)	63.3	2.22 (0.876) <sup>b</sup>	2.17	0.420 <sup>c</sup>	7.1
320	0.48	23.0	1.76 (0.937)	1.89 (1.077)	23.9	1.75 (0.937)	46.9	1.72 (0.946)	1.68	0.326 <sup>c</sup>	9.2
338	0.43	12.3	1.38 (1.249)	1.50 (0.519)	8.44	1.40 (1.237)	15.1	1.47 (0.511)	1.40	0.261 <sup>c</sup>	11.5
356	0.34	7.05	0.596 (1.115)	0.697 (0.529)	7.85	0.590 (1.114)	12.1	0.651 (0.472)	0.628	0.117 <sup>d</sup>	25.6
385	0.14	3.17	0.166 (0.725)	0.207 (0.515)	6.11	0.148 (0.678)	8.05	0.164 (0.355)	0.163	0.030 <sup>d</sup>	100

<sup>a</sup>No. of C-C bonds in a flexible subchain

$$^b \text{R.m.s. error} = \frac{100}{y_{0,\text{exp}}} \times \left( \frac{s}{n + \frac{1}{2}} \right)^{\frac{1}{2}} \text{ with } s = \frac{1}{2}(y_{0,\text{exp}} - y_{0,\text{calc}})^2 + \sum_{i=1}^n (y_{i,\text{exp}} - y_{i,\text{calc}})^2$$

<sup>c</sup>Gaussian shape of dipolar broadening function S

<sup>d</sup>Lorentzian shape of dipolar broadening function S

(from 1 to 0.68), and very steeply beyond this range, reaching zero at 90°. Without implying the validity of the cone model for internal motion in amorphous polyethylene, the values  $\omega_{2\text{ res}}:\omega_{2\text{ RL}}$  nevertheless indicate that the amplitude of the motion of each methylene proton pair must be relatively large even at the lowest temperature studied. Equation (1), as formulated in the Introduction, implies spatially hindered internal motion where the inter-proton vector can, within some limits (e.g. the cone angle  $\alpha_0$ ), randomly assume orientations symmetrically distributed about some specified direction, with a random distribution of these directions ( $\theta$  angles, cone axes). It ignores any distribution in the degree of motional hindrance, as characterized by the parameter  $A_{0G}$  (or cone angle  $\alpha_0$ ). However, it has been shown in our previous communications<sup>3,22</sup> that lineshapes governed by a random distribution of the angles  $\theta$  are not very sensitive to the presence of any further distribution. As the Lorentzian shape can be represented as a certain distribution of Gaussians<sup>3</sup>, the better fit obtained with a Lorentzian than with a Gaussian shape of the function S at elevated temperatures might be a manifestation of a distribution in the degree of motional hindrance.

The temperature dependence of  $A_{0G}$ , as a parameter characteristic of spatial restrictions of motion, cannot be discussed in terms of activation energy on grounds similar to those discussed for the order parameter S by English<sup>21</sup>.  $A_{0G}$  gives a linear plot vs.  $T^2$  (Figure 5), extrapolating to 0 at 113.7°C. For our sample, this is the 'n.m.r. melting temperature', defined so that at this point all 'near-static' dipolar interactions (with  $\nu_c < 10^3$  Hz) disappear. (The internal motion may remain anisotropic even above this point but this 'melt' anisotropy would be manifested in a range of higher frequencies.)

In our previous studies of swollen chemically crosslinked polymer gels<sup>1-3</sup>, the width of the dipolar broadening function was found to be almost independent of temperature, and to depend on the degree of crosslinking. For swollen crosslinked polystyrenes, the parameter  $A_{0G}$  was found<sup>2</sup> to be inversely proportional to the mean number of C-C bonds between two crosslinks.

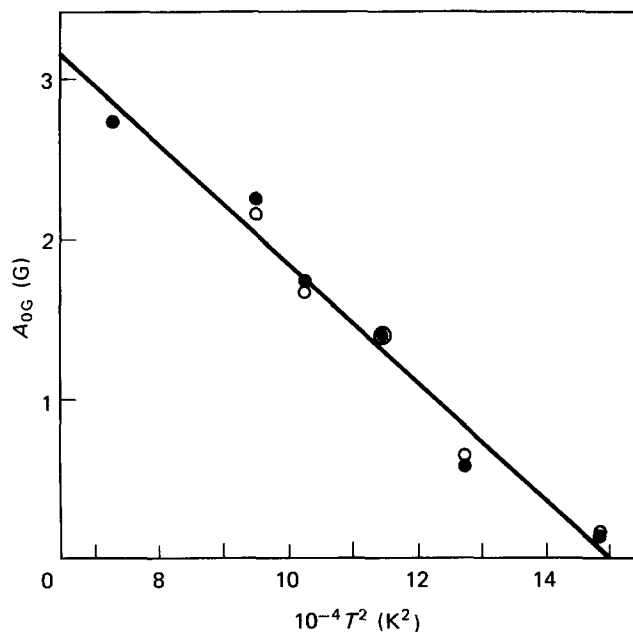


Figure 5 Temperature dependence of the dipolar broadening parameter  $A_{0G}$ , obtained with Gaussian (●) or Lorentzian (○) shape of function S

In the amorphous phase of polyethylene, motional hindrance is caused by physical crosslinks which can be represented both by the crystallites fixing the ends of the amorphous portions of the chains, and by physical constraints (e.g. entanglements, tube constraints, etc.) within the amorphous phase itself. Unlike chemical crosslinks, such physical constraints are expected to be temperature-dependent, explaining the strong temperature dependence of  $A_{0G}$ . Considering only the methylene proton pair interaction, as the largest single contribution to the second moment, the mean length of the flexible subchains can be estimated by means of the approximate formula of Gotlib<sup>23</sup>:

$$Q \equiv \omega_{2\text{ res}}/\omega_{2\text{ RL}} = 3/10z$$

where  $z$  is the number of statistical segments. Setting the length of the statistical segment of polyethylene equal to 10 C–C bonds<sup>24</sup>, the mean number of C–C bonds in a flexible subchain can be estimated as  $n = 10z \approx 3/Q$ . The numbers in the last column of *Table 1* indicate that the length of the flexible subchain in our LDPE sample at room temperature is of the order of seven C–C bonds, i.e. much shorter than would correspond to an inter-crystallite link in an amorphous layer of thickness  $\sim 70$  Å. Therefore the main contribution to the width of the dipolar broadening function comes from physical constraints in the amorphous layer itself. The numbers  $n$  in *Table 1* agree reasonably well with the results of <sup>2</sup>H n.m.r. studies of a deuterated linear PE sample<sup>25,26</sup>, where anisotropy of internal motion in the amorphous phase was also characterized, and the length of the mobile segment was determined as three bonds at 193 K (75% crystallinity) and 10–15 bonds at 383 K ( $\sim 55\%$  crystallinity).

### CONCLUSIONS

The present study demonstrates that the <sup>1</sup>H n.m.r. amorphous lineshape of LDPE can be described by assuming the presence of only a single amorphous phase. Its dynamics are similar to those of gels of chemically crosslinked polymer networks. Rapid conformational motions are spatially hindered by the presence of physical crosslinks, represented not only by the crystallites but mostly by physical constraints within the amorphous phase itself. Contrary to chemically crosslinked networks, the number of physical crosslinks rapidly decreases with increasing temperature; spatial restrictions of motion with a lifetime longer than  $10^{-3}$  s disappear completely in the vicinity of the melting temperature.

### REFERENCES

- 1 Doskočilová, D., Schneider, B. and Jakeš, J. *Polymer* 1980, **21**, 1185
- 2 Schneider, B., Doskočilová, D. and Dybal, J. *Polymer* 1985, **26**, 253
- 3 Doskočilová, D. and Schneider, B. *Pure Appl. Chem.* 1982, **54**, 575
- 4 Schneider, B., Jakeš, J., Pivcová, H. and Doskočilová, D. *Polymer* 1979, **20**, 939
- 5 Bergmann, K. and Nawotki, K. *Kolloid Z.-Z. Polym.* 1967, **219**, 132
- 6 Bergmann, K. *J. Polym. Sci., Polym. Phys. Edn.* 1978, **16**, 1611
- 7 Bergmann, K. *Polym. Bull.* 1981, **5**, 355
- 8 Schneider, B., Pivcová, H. and Doskočilová, D. *Macromolecules* 1972, **5**, 120
- 9 Flory, P. J. *Pure Appl. Chem.* 1984, **56**, 305
- 10 Spěváček, J. *Polymer* 1978, **19**, 1149
- 11 Stokr, J., Růžička, Z. and Ekwil, S. R. *J. Appl. Spectrosc.* 1974, **28**, 479
- 12 Schneider, B., Doskočilová, D., Babka, J. and Růžička, Z. *J. Magn. Res.* 1978, **29**, 79
- 13 Kakudo, M. and Ullman, R. *J. Polym. Sci.* 1960, **45**, 91
- 14 Gopalan, M. R. and Mandelkern, L. *J. Polym. Sci.* 1967, **5B**, 925
- 15 Stein, R. S. and Sutherland, G. B. M. *J. Chem. Phys.* 1954, **22**, 1993
- 16 Hendus, H. and Schnell, G. *Kunststoffe* 1961, **51**, 69
- 17 Strobl, G. R., Schneider, M. J. and Voigt-Martin, I. G. *J. Polym. Sci., Polym. Phys. Edn.* 1980, **18**, 1361
- 18 Voigt, G. and Kimmich, R. *Polymer* 1980, **21**, 1001
- 19 Kimmich, R. and Bachus, R. *Colloid Polym. Sci.* 1982, **260**, 911
- 20 Lipari, G. and Szabo, A. *J. Am. Chem. Soc.* 1982, **104**, 4546
- 21 English, A. D. *Macromolecules* 1984, **17**, 2182
- 22 Jakeš, J. *Collect. Czech. Chem. Commun.* 1983, **48**, 2028
- 23 Gotlib, J. J., Lifshitz, M. I., Shevelev, V. A., Lishanski, I. S. and Balanina, I. V. *Vysokomol. Soed.* 1976, **18A**, 2299
- 24 Flory, P. J. 'Statistical Mechanics of Chain Molecules', John Wiley, New York, 1969
- 25 Hentschel, D., Sillescu, H. and Spiess, H. W. *Polymer* 1984, **25**, 1078
- 26 Spiess, H. W. *Colloid Polym. Sci.* 1983, **261**, 193